the FEBS Journal

A short-chain dehydrogenase involved in terpene metabolism from *Zingiber zerumbet*

Sho Okamoto[1,*], Fengnian Yu[1,*], Hisashi Harada[2], Toshihide Okajima[3], Jun-ichiro Hattan[4], Norihiko Misawa[2,4] and Ryutaro Utsumi[1]

1 Department of Bioscience, Graduate School of Agriculture, Kinki University, Nara, Japan
2 Central Laboratories for Frontier Technology, Kirin Holdings Co. Ltd., Ishikawa, Japan
3 Institute of Scientific and Industrial Research, Osaka University, Japan
4 Research Institute for Bioresources and Biotechnology, Ishikawa Prefectural University, Japan

Keywords
bisubstrate; short-chain dehydrogenase-reductase; zerumbone; *Zingiber zerumbet* Smith; ZSD1

Correspondence
R. Utsumi, Department of Bioscience, Graduate School of Agriculture, Kinki University, Nakamachi, Nara 631-8505, Japan
Fax: +81 742 43 8976
Tel: +81 742 43 7306
E-mail: utsumi@nara.kindai.ac.jp

*These authors contributed equally to this work

(Received 27 February 2011, revised 20 May 2011, accepted 7 June 2011)

doi:10.1111/j.1742-4658.2011.08211.x

The rhizome oil of *Zingiber zerumbet* Smith contains an exceptionally high content of sesquiterpenoids with zerumbone, a predominating potential multi-anticancer agent. Biosynthetic pathways of zerumbone have been proposed, and two genes *ZSS1* and *CYP71BA1* that encode the enzymes catalyzing the first two steps have been cloned. In this paper, we isolated a cDNA clone (*ZSD1*) that encodes an alcohol dehydrogenase capable of catalyzing the final step of zerumbone biosynthesis. *ZSD1* has an open reading frame of 804 bp that encodes a 267-residue enzyme with a calculated molecular mass of 28.7 kDa. After expression in *Escherichia coli*, the recombinant enzyme was found to catalyze 8-hydroxy-α-humulene into zerumbone. ZSD1 is a member of the short-chain dehydrogenase/reductase superfamily (SDR) and shares high identities with other plant SDRs involved in secondary metabolism, stress responses and phytosteroid biosynthesis. In contrast to the transcripts of *ZSS1* and *CYP71BA1*, which are almost exclusively expressed in rhizomes, *ZSD1* transcripts are detected in leaves, stems and rhizomes, suggesting that ZSD1 may also be involved in other biological processes. Consistent with its proposed flexible substrate-binding pocket, ZSD1 also converts borneol to camphor with K_m and k_{cat} values of 22.8 μM and 4.1 s^{-1}, displaying its bisubstrate feature.

Introduction

Zingiber zerumbet Smith, a member of the Zingiberaceae family, is widely cultivated for its medicinal properties throughout the tropics and the subtropics, particularly in Southeast Asia. The rhizome of *Z. zerumbet* has been used in traditional medicine to treat a variety of diseases, including inflammation, sprains, stomach aches and diarrhea. Its special aromatic odor is due to the complex mixture of the monoterpenoids and sesquiterpenoids in its rhizome essential oil. Although the composition of the rhizome oil of *Z. zerumbet* shows variations among different ecotypes [1–5], the most abundant and characteristic component is zerumbone, a pharmaceutically interesting sesquiterpenoid. In recent decades, zerumbone has attracted intensive attention for its anti-inflammatory [6] and multiple anticancer properties [7–11].

It has been assumed that the biosynthetic pathway of zerumbone in *Z. zerumbet* from the common sesquiterpene precursor farnesyl diphosphate is analogous to the biosynthesis of other plant terpene ketones [12,13]

Abbreviations
GatDH, galactitol dehydrogenase; 8-HAH, 8-hydroxy-α-humulene; SDR, short-chain dehydrogenase/reductase.

(Fig. 1). Two genes, *ZSS1* and *CYP71BA1*, encoding α-humulene synthase and α-humulene-8-hydoxylase, respectively, which are proposed to be responsible for the two early committed steps of zerumbone biosynthesis, have been cloned and characterized [14,15]. The final step was assumed to be catalyzed by a short-chain dehydrogenase.

Short-chain dehydrogenases/reductases (SDRs) are highly divergent NAD(P)(H)-dependent enzymes with typically about 250 amino acid residues [16]. They cover a wide range of substrate spectra, ranging from alcohols, steroids, sugars and aromatic compounds to xenobiotics [17]. In plants, SDRs participate in many important biochemical and physiological processes, such as secondary metabolism [18], stress responses [19] and phytosteroid biosynthesis [20]. In terpenoid metabolism, SDRs are one of the most important terpene-modifying enzymes for catalyzing oxidation/reduction reactions, which are crucial for the synthesis of biologically active terpenoid molecules. In mint, two similar short-chain dehydrogenases and two reductases involved in monoterpenoid biosynthesis have been reported [21,22]. Recently, a multisubstrate monoterpene alcohol dehydrogenase and a terpenoid reductase have also been characterized from *Artemisia annua* [23,24]. To elucidate the final step of the zerumbone biosynthesis, a homology-based cloning strategy was employed to clone short-chain alcohol dehydrogenase genes from *Z. zerumbet* rhizomes. Here, we describe the isolation and the functional characterization of a cDNA clone encoding an alcohol dehydrogenase that can convert both 8-hydroxy-α-humulene (8-HAH) to zerumbone and monoterpene alcohol borneol to camphor.

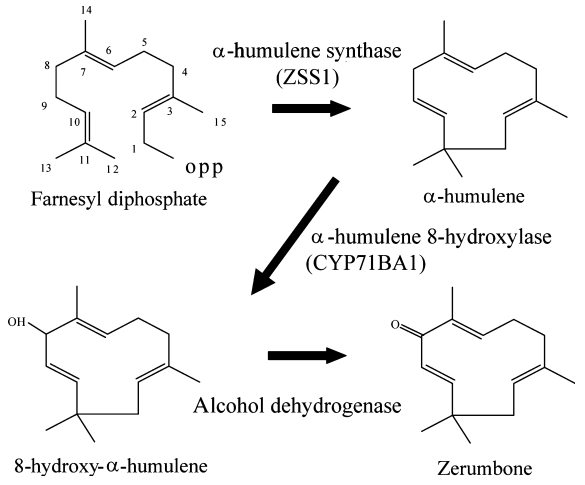

Fig. 1. Proposed pathway for zerumbone biosynthesis in *Z. zerumbet*.

Results and Discussion

Homology-based cloning of *ZSD1* encoding a dehydrogenase from rhizomes of *Z. zerumbet*

Plant SDRs are one of the most important terpene-modifying enzymes that catalyze oxidation/reduction reactions [21–24]. Although there has been increasing evidence that a multifunctional cytochrome P450 can catalyze the successive conversion of terpene hydrocarbons to the corresponding ketones [25,26], our previous studies showed that CYP71BA1 cannot catalyze the successive reactions from α-humulene to zerumbone [15]. Therefore, we assumed that the final step is the oxidation of 8-HAH to zerumbone by an alcohol dehydrogenase.

In an effort to isolate dehydrogenase cDNA from *Z. zerumbet*, RT-PCR was conducted using two degenerate primers designed on the highly conserved regions of plant SDRs (Fig. 2), and a predominant fragment with the predicated length of approximately 350 bp was generated. After sequencing, this fragment showed a high similarity to known SDRs. Then, a combination of 5′RACE and 3′RACE was performed using specific primers to obtain the remaining 5′ and 3′ sequences. Two different types of full-length cDNA clones were obtained. One of them, named *ZSD1*, has an ORF of 804 bp that encodes a 267-residue enzyme with a calculated molecular mass of approximately 28.7 kDa and an isoelectric point of 5.63 calculated from the deduced amino acid sequence (Fig. S1) (accession no. AB480831). ZSD1 contains a NAD^+-binding motif (TGxxxGxG), a downstream structural domain ((N/C)NAG) of undefined function and an active site sequence (YxxxK), indicating that it belongs to the 'classical' subfamily of the SDR superfamily [16] (Fig. S1). A BLAST search of the GenBank database demonstrated that ZSD1 is most closely related to several putative alcohol dehydrogenases of other plant species with the highest identity 65%. Among the functionally characterized enzymes, ZSD1 is shown to be highly similar to SDRs involved in abscisic acid biosynthesis with identities of 61% (*Citrus sinensis*), 59% (*Solanum tuberosum*) and 56% (*Arabidopsis thaliana*). Interestingly, significant homology is also observed with *Digitalis lanata* 3-β-hydroxysteroid dehydrogenase (48% identity) [20]. However, phylogenetic analysis revealed its distant relationship to several known terpene-modifying SDRs, such as *Mentha* × *piperita* isopiperitenol dehydrogenase (35% identity), its menthol dehydrogenase (14% identity) [27] and *Aedes aegypti* farnesol dehydrogenase (25% identity) [28] (Fig. 2).

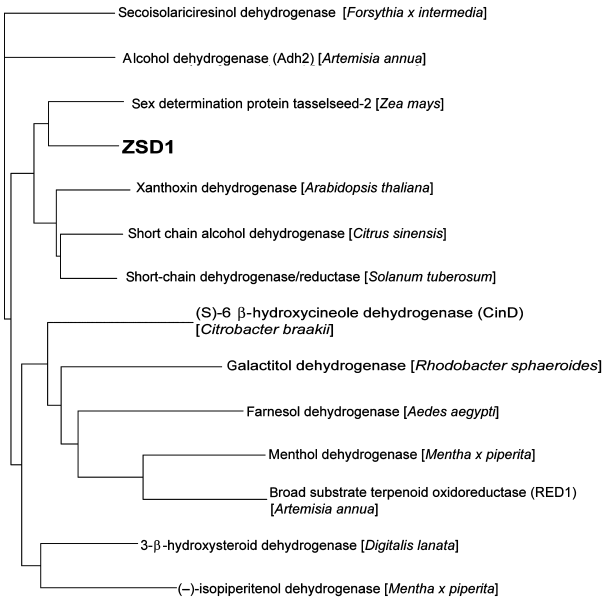

Fig. 2. Phylogenetic analysis of ZSD1 and related functionally characterized SDRs. The tree was constructed using the neighbor-joining algorithm with CLUSTALW (http://align.genome.jp/) and visualized with TREEVIEW. Sequences and associated GenBank accession numbers are *Forsythia* × *intermedia* secoisolariciresinol dehydrogenase (AAK38665), *Artemisia annua* alcohol dehydrogenase (ADK56099), *Zea mays* sex determination protein tasselseed-2 (ACG37730), *Zingiber zerumbet ZSD1* (AB480831), *Arabidopsis thaliana* xanthoxin dehydrogenase (NP_175644), *Citrus sinensis* short-chain alcohol dehydrogenase (ADH82118), *Solanum tuberosum* short-chain dehydrogenase/reductase (AAT75153), *Citrobacter braakii* (*S*)-6β-hydroxycineole dehydrogenase (GQ849481), *Rhodobacter sphaeroides* galactitol dehydrogenase (ACM89305), *Aedes aegypti* farnesol dehydrogenase (GQ344797), *Mentha* × *piperita* menthol dehydrogenase (AAQ55960), *Artemisia annua* broad substrate reductase/dehydrogenase (RED1) (GU167953), *Digitalis lanata* 3β-hydroxysteroid dehydrogenase (CAC936678), and *Mentha* × *piperita* (–)-isopiperitenol dehydrogenase (AAU20370).

ZSD1 catalyzes 8-HAH to zerumbone *in vitro*

To examine whether ZSD1 could catalyze the conversion of 8-HAH to zerumbone, the full-length *ZSD1* was expressed in *Escherichia coli* BL21 (DE3) and the recombinant protein was purified by Ni-affinity chromatography. Then, the purified protein was incubated with 8-HAH in the presence of NAD^+ or $NADP^+$, and the product was analyzed by GC-MS. As shown in Fig. 3, a single product peak matching the authentic standard of zerumbone was generated when NAD^+ was used as cofactor, whereas no product was detected in the presence of $NADP^+$ (data not shown). Therefore, ZSD1 is a NAD-dependent dehydrogenase capable of oxidizing the C8 hydroxyl group of 8-HAH to form zerumbone.

ZSD1 transcript accumulation is detected in leaves, stems and rhizomes

The total RNA from leaf, stem and rhizome tissues of *Z. zerumbet* was extracted, and quantitative real-time PCR analysis was performed to examine the mRNA levels of *ZSD1* in different tissues. A partial cDNA sequence of ubiquitin was used as an internal reference. The results showed that ZSD1 is highly expressed in all of the tissues examined (Fig. 4A). This finding is surprising in that zerumbone is only present in rhizomes of *Z. zerumbet*, and transcripts of *ZSS1* and *CYP71BA1* encoding the two upstream enzymes of zerumbone biosynthesis are almost exclusively accumulated in rhizomes (Fig. 4B,C) [15]. Thus, in addition to converting 8-HAH to zerumbone, ZSD1 may also contribute to the dehydrogenation reactions of other compounds as well.

ZSD1 also converts borneol to camphor *in vitro*

To explore the possibility that ZSD1 also participates in dehydrogenation reactions of other compounds, the enzyme assay was carried out using borneol as a substrate based on the fact that trace amounts of borneol and high content of camphor are found in *Z. zerumbet*. As shown in Fig. 5A, borneol was efficiently converted to camphor by ZSD1, confirming that ZSD1 may have a broad substrate specificity. In this regard, ZSD1 is similar to Adh2, a recently characterized monoterpenoid alcohol dehydrogenase from *A. annua* that exhibits dehydrogenase activity with several monoterpene alcohol substrates including borneol [23].

Kinetic comparisons of ZSD1 for different substrates

Because ZSD1 can act on both 8-HAH and borneol, we conducted a kinetic analysis to evaluate the catalytic preferences of ZSD1 for these two different substrates. As shown in Table 1, the recombinant ZSD1 selectively uses NAD^+ but not $NADP^+$ as a cofactor and the K_m value for NAD^+ is 27.3 μM with a k_{cat} value of 3.8 s^{-1} at pH 8.0. While the K_m and k_{cat} values for borneol are 22.8 μM and 4.1 s^{-1}, respectively, the k_{cat}/K_m value for 8-HAH is lower than for borneol. Thus, it is likely that ZSD1 has a substrate preference for borneol over 8-HAH. Nevertheless, the relatively lower catalytic efficiency of ZSD1 for that of 8-HAH *in vitro* may be at least partially due to the poorer solubility of 8-HAH in the aqueous reaction solution. The high content of zerumbone and trace amounts of 8-HAH in rhizomes of *Z. zerumbet* suggest that the rate of conversion is sufficient *in vivo*.

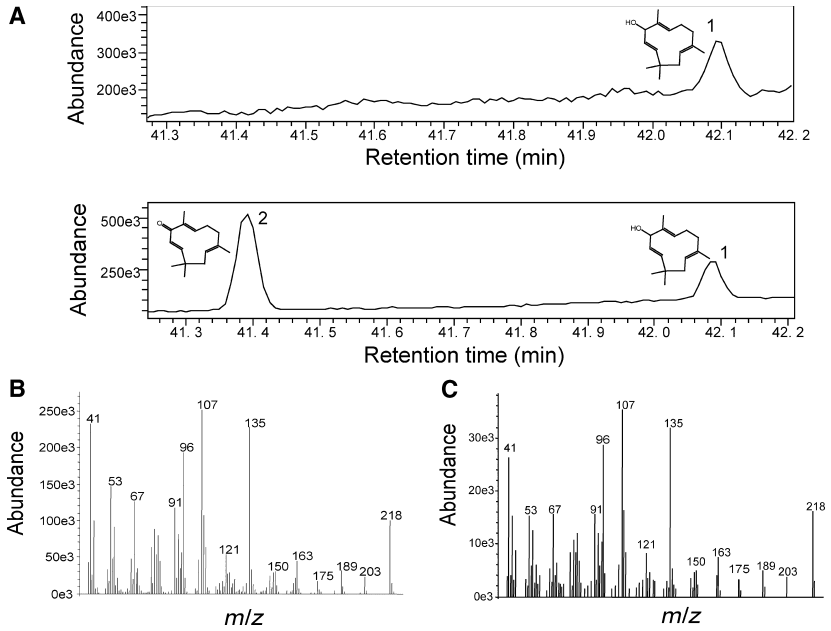

Fig. 3. GC-MS analysis of products generated by recombinant ZSD1 with 8-HAH as substrate. (A) Chromatogram of products formed by incubation of 8-HAH with proteins from *E. coli* cells carrying the empty expression vector (pET101). Peak 1, 8-HAH. (B) Chromatogram of products generated by incubation of 8-HAH with recombinant ZSD1. Peak 2, zerumbone. (C) Mass spectrum of peak 2. (D) Mass spectrum of authentic zerumbone.

However, we cannot rule out the possibility that a dehydrogenase distinct from ZSD1 can catalyze zerumbone formation in *Z. zerumbet*.

A 3D structure model of ZSD1 reveals a large, flexible substrate-binding pocket

The bisubstrate property of ZSD1 led us to perform molecular modeling studies on it to obtain structural insights. A 3D structural model of ZSD1 was constructed by homology modeling based on the crystal structure of *Podophyllum peltatum* (–)-secoisolariciresinol dehydrogenase [29] (PDB code 2BGK) and superimposed onto *Rhodobacter sphaeroides* galactitol dehydrogenase (GatDH) [30] (PDB code 3LQF), whose co-crystal structure with NAD^+ and an alcohol substrate is known (Fig. 6). Common to most alcohol dehydrogenases, ZSD1 displays a typical Rossmann-fold dinucleotide cofactor-binding motif, a Tyr-based catalytic center with adjacent Ser and Lys residues, and a substrate-binding site that is mainly surrounded by hydrophobic residues (Fig. 6A). Superimposition of ZSD1 on GatDH reveals that the two structures are nearly identical in the N-terminal segments, despite their low sequence identity (30%). However, in the highly variable C-terminal region, a much larger and flexible substrate-binding pocket was observed in ZSD1, which may allow it to accommodate multiple substrates, thereby conferring its versatile functional property (Fig. 6B).

Ser142 completes the Ser-Tyr-Lys triad responsible for the catalysis of ZSD1

It is well known that many SDR family members utilize a highly conserved Ser-Tyr-Lys triad (Ser and

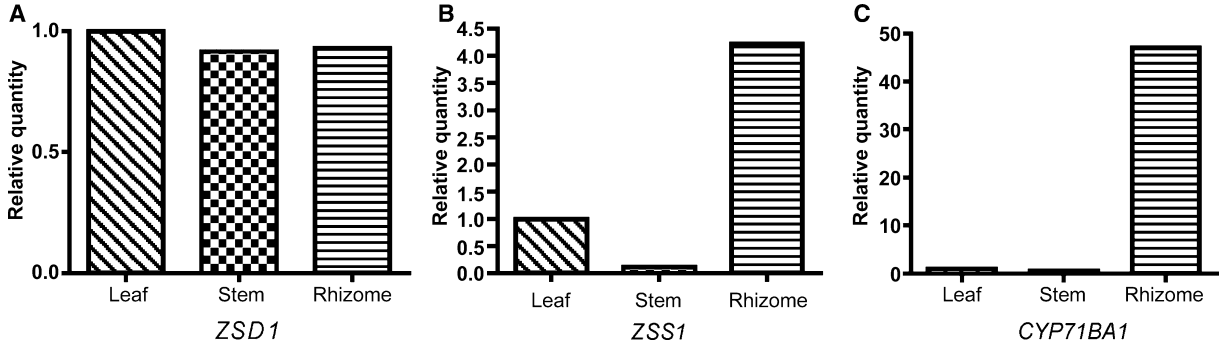

Fig. 4. Tissue-specific expression profiles of ZSD1, ZSS1 and CYP71BA1. Quantitative RT-PCR analysis of ZSD1 (A), ZSS1 (B) and CYP71BA1 (C) transcript levels in leaves (oblique line), stems (checked) and rhizomes (striped). Ubiquitin was used as a reference gene.

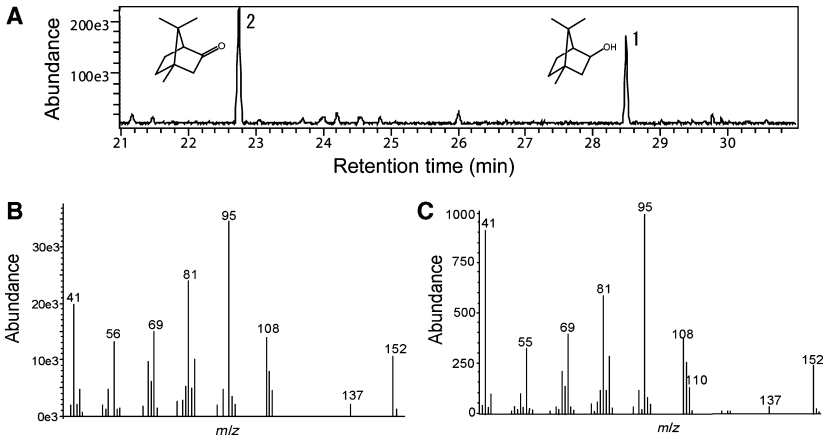

Fig. 5. GC-MS analysis of products in the enzyme assay using borneol. (A) Chromatogram of products formed by incubation of borneol with recombinant ZSD1. Peak 1, borneol; peak 2, camphor. (B) Mass spectrum of peak 2. (C) Mass spectrum of authentic camphor.

Table 1. Kinetic parameters for recombinant wild-type ZSD1 and four mutants. ND, enzymatic activity was not detected.

	NAD^+			8-HAH			Borneol		
	K_m (μM)	k_{cat} (s^{-1})	k_{cat}/K_m ($\mu M^{-1}\cdot s^{-1}$)	K_m (μM)	k_{cat} (s^{-1})	k_{cat}/K_m ($\mu M^{-1}\cdot s^{-1}$)	K_m (μM)	k_{cat} (s^{-1})	k_{cat}/K_m ($\mu M^{-1}\cdot s^{-1}$)
Wild-type	27.3	3.8	1.39×10^{-1}	58.5	1.3	2.2×10^{-2}	22.8	4.1	1.79×10^{-1}
Y155A	43.7	0.1	2.0×10^{-3}	78.2	0.1	1.0×10^{-3}	55.1	0.1	2×10^{-3}
K159A	ND	ND	ND	ND	ND	ND	ND	ND	ND
S142A	121	0.1	8.0×10^{-4}	138	0.1	7.0×10^{-4}	111	0.1	9×10^{-4}
S144A	16.1	4.4	2.62×10^{-1}	28.1	2.9	1.03×10^{-1}	13.2	4.5	3.41×10^{-1}

YXXXK motif) to perform the oxidoreductase enzyme reaction, with Tyr residue acting as the catalytic base [31]. Since sequence analysis of ZSD1 has revealed a similar motif ($_{155}$Y-X-X-X-K_{159}) (Fig. 2), we assume that Tyr155 and Lys159 residues are predicted to be the possible catalytic residues as reported previously. Site-directed mutagenesis and steady-state kinetic analysis showed that the k_{cat}/K_m value of Y155A mutant enzyme for the three substrates decreased to approximately 1/20 to 1/50 of the wild-type ZSD1, while K159A mutant exhibited no ZSD1 activity at all (Table 1) [32]. These observations confirmed the key roles for Tyr155 and Lys159 in the catalytic function of ZSD1.

Because our homology model of ZSD1 shows that Ser142 and Ser144 are localized in close proximity to Tyr155 (Fig. 6A), we also created the mutants S142A and S144A by PCR-based mutagenesis in order to identify the third member of the catalytic triad. Kinetic analysis indicated that the catalytic efficiency (k_{cat}/K_m) of the S142A mutant for all three substrates was remarkably reduced (1/200-1/20 fold) compared with the wild-type ZSD1. In contrast, the k_{cat}/K_m values of the S144A mutant increased 2–5 fold (Table 1). These results strongly suggest that Ser142 completes the catalytic triad (Ser142-Tyr155-Lys159) responsible for ZSD1 activity for 8-HAH and borneol. Since ZSD1 has 16 Ser residues, this result also validates the accuracy of our homology model. The unexpected finding that the mutation of Ser144 enhances the catalytic efficiency of ZSD1 provides a possibile way to improve the yield of products such as zerumbone by mutagenesis, although further studies are required to understand why the S144A mutant results in improved enzyme efficiency.

In conclusion, we cloned and characterized a bisubstrate SDR (ZSD1) from *Z. zerumbet*, which acts on both sesquiterpene alcohol 8-HAH and monoterpene alcohol borneol. Its broad expression pattern and its proposed flexible substrate-binding pocket are consistent with its bisubstrate property.

Experimental procedures

Plant materials and chemicals

Samplings of ginger plants (*Zingiber zerumbet* Smith) provided by Sakata Co. (Kochi, Japan) were grown in a greenhouse under natural light and environmental conditions. Mid-summer plants were used for the cDNA cloning. Rhizomes, stems and leaves for analysis of the gene expression were harvested in different seasons, immediately frozen in liquid N_2, and stored at −80 °C for RNA isolation. 8-HAH was obtained from the Nard Institute Ltd (Hyogo, Japan). α-humulene and other reagents were purchased from Sigma and Aldrich Chemical Co (St. Louis, CA, USA).

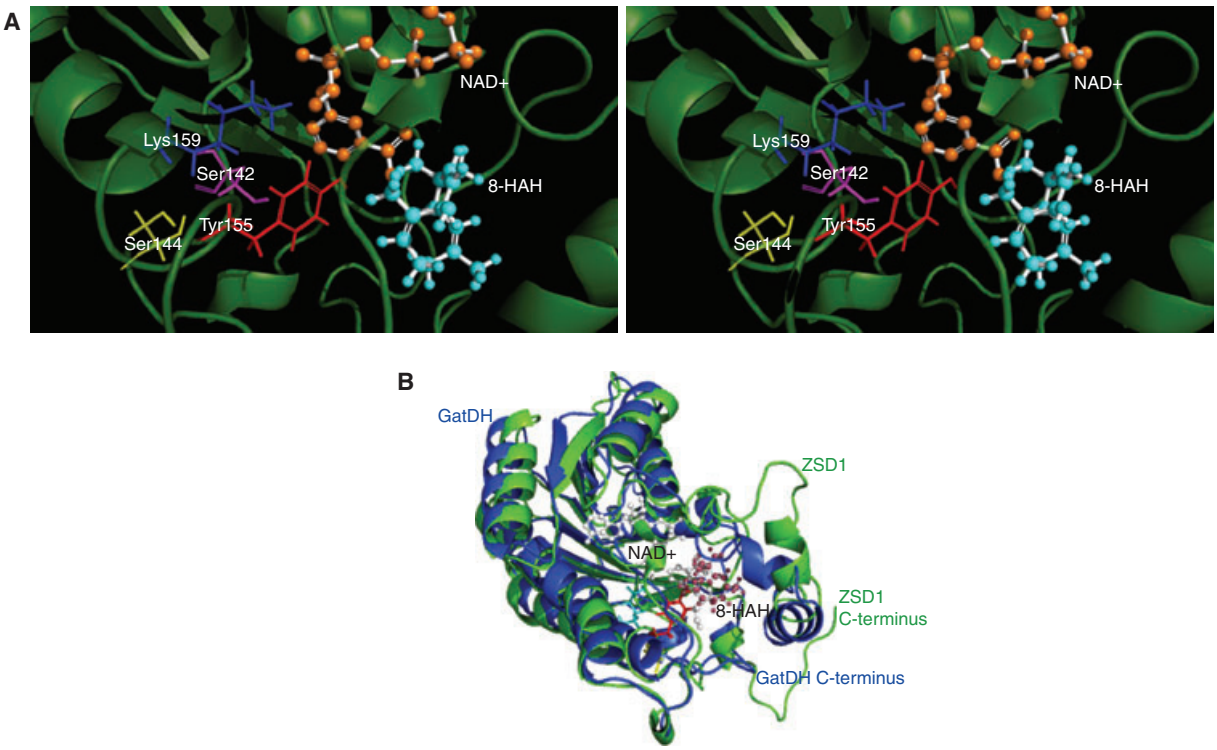

Fig. 6. (A) 3D structure model of monomeric ZSD1 in stereo. The NAD+ and 8-HAH structures are included. The catalytic Tyr155 (red) and Lys159 (blue) residues as well as the potentially catalytic Ser142 (magenta) and Ser144 (yellow) residues are shown. (B) 3D structure model of monomeric ZSD1 with NAD and 8-HAH is superimposed on monomeric GatDH (PDB code 3LQF). Green ribbon model indicates ZSD and blue ribbon model indicates GatDH 3D structure.

Isolation of *ZSD1* cDNA

Total RNA from rhizomes for RT-PCR was isolated with a Spectrum Plant Total RNA Kit (Sigma-Aldrich, St. Louis, CA, USA). Three micrograms of RNA were reverse transcribed into cDNA in a 20-μL reaction with poly(dT) priming using a SuperScript III First-Strand Synthesis Kit (Invitrogen). Two degenerate primers, 5′-GGIAARGTI GCCHTIRTVACIGG-3′ (forward) and 5′-GGRCTNAC RCARTTIACIC-3′ (reverse), were used for RT-PCR. The PCR conditions were adjusted as follows: denaturation at 94 °C for 2 min, followed by 35 cycles of 94 °C for 30 s, 51 °C for 30 s, 72 °C for 30 s, and a final extension at 72 °C for 2 min. The PCR products were purified and cloned into a pGEM-T Easy Vector (Promega, Madison, WI, USA) and introduced into *E. coli* DH5α cells. The cDNA clones were sequenced using BigDye Terminator version 3.1 (Applied Biosystems, Foster City, CA, USA) and an ABI3100 sequencer (Applied Biosystems). The molecular cloning experiments in this study were mainly performed based on Sambrook *et al.* (1989, Molecular cloning: a laboratory manual. Cold Spring Harbor Laboratory, Cold Spring Harbor, New York.). To isolate full-length cDNA, the partial sequence was extended toward the 5′- and 3′-end with the Smart RACE cDNA Amplification Kit (Takara Bio, Ohtsu, Japan) following the manufacturer's protocol. The following two gene-specific primers were used for RACE: 5′-CGGATGTCAATGACCTTG TCACCTGT-3′ for 5′RACE and 5′-GATGAGCTTGGTC AGCAAGTAAGCCAAC-3′ for 3′RACE. The PCR products were cloned into pGEM-T Easy Vector (Promega) and analyzed to determine the nucleotide sequence of the ORF in the cDNA. The cDNA fragment containing the entire ORF from the initial codon (ATG) to the terminal codon (TGA) for *ZSD1* was then amplified by PCR using a prime star HS DNA polymerase (Takara Bio, Ohtsu, Japan) with a pair of oligonucleotide primers (5′-ATGAGGTTAGA AGGGAAAGTTGC-3′ and 5′-TTCGAACACTTGGAGT GTATGG-3′) according to the manufacturer's instructions. The deduced amino acid sequences of selected SDRs were aligned using the neighbor-joining algorithm with CLUSTALW (http://align.genome.jp/). The phylogenetic tree was visualized using TREEVIEW software.

Bacterial expression and enzyme assay

The amplified full-length product was cloned into a pET101/DTOPO vector (Invitrogen) to express *ZSD1* as a His-tagged protein. The recombinant plasmid pET-ZSD1 was transformed into *E. coli* TOP10F cells for sequence

characterization and into *E. coli* BL21 (DE3) for expression. For functional expression, recombinant *E. coli* cells were grown to OD_{600} = 0.5–0.6 at 37 °C and Luria broth medium containing ampicillin (100 μg·mL^{-1}). Cultures were then induced by adding isopropyl-β-D-thiogalactopyranoside to a final concentration of 1 mM and grown for another 3.5 h at 37 °C. The cells were collected by centrifugation and stored at −80 °C until used. The frozen cells were suspended in a chilled lysis buffer (50 mM Tris/HCl (pH 8.0), 100 mM NaCl) containing 1 mM phenylmethylsulphonyl fluoride and disrupted with a sonicator (Branson advanced digital sonifier 250DA). The lysates were cleared by centrifugation and filtered through a 0.45-μm filter. The filtrate was loaded onto a HisTrap HP column (ÄKTA prime system; GE Healthcare Bio-Science, Piscataway, NJ, USA) equilibrated with the lysis buffer, and the His6 protein was eluted using an imidazole gradient from 0 to 500 mM. The protein eluate was further desalted into an assay buffer (20 mM KH_2PO_4, pH 7.0, 7.5 and 8.0) by passage through an Econopac column (Bio-Rad, Hercules, CA, USA), and the resulting enzyme eluate was used for the enzyme assay. Each assay was done in a volume of 1 mL with 20 mM KH_2PO_4, pH 7.0, 865 μL of enzyme, 1 mM NAD, 10 mM EDTA and 0.1 mM 8-HAH, borneol or pregnenolone. After overnight incubation at 37 °C, the mixture was extracted with pentane (3 × 1 mL) and concentrated to a minimum volume for GC-MS analysis. Gel permeation chromatography of the recombinant ZSD1 was conducted on a calibrated Sephadex 200 (GE Healthcare, Amersham Place, UK) column with 50 mM KH_2PO_4, pH 8.0, containing 150 mM NaCl as running buffer at a flow rate of 0.5 mL·min^{-1}.

Product identification

GC-MS analysis of terpenoids was performed on a Shimadzu QP5050A GC/MS system with a DB-WAX column (0.25 mm internal diameter × 0.25 μm film thickness × 30 m; Agilent Technologies, Santa Clara, CA, USA). Split injections (1 × l) were made at a ratio of 22 : 1 with an injector temperature of 250 °C. The instrument was programmed from an initial temperature of 40 °C (held for 3 min) and increased at 3 °C·min^{-1} until 80 °C, 5 °C·min^{-1} until 180 °C, and 10 °C·min^{-1} until 240 °C (held for 5 min). Helium was used at a constant flow of 1.8 mL·min^{-1}. Mass spectra were measured with a mass range *m/z* of 40–400, an electron voltage of 70 eV and an interface temperature of 230 °C.

Enzyme characterization

Michaelis–Menten kinetic parameters for 8-HAH and borneol were determined using purified wild-type enzymes and four mutants. A kinetics assay was done in a volume of 1 mL with 20 mM KH_2PO_4 (pH 8.0), 200 μL of enzyme, 1 mM NAD and 10 mM EDTA by changing the concentration of substrates or NAD^+ systematically, while maintaining the other reactant at saturation. The reaction was monitored at 37 °C by absorbance at 340 nm. K_m (Michaelis–Menten constant) and V_{max} (maximal reaction velocity) were calculated from at least eight measurements by linear regression from double-reciprocal plots. The k_{cat} values (s^{-1}) were calculated from the V_{max} values and represent the maximal turnover rate. pH optimum was measured using the same buffer system over a pH range of 7.0–8.0 at 0.5 pH intervals.

Transcript expression analysis

Possible traces of DNA were removed using Turbo DNA-free™ kit (Ambion, Austin, TX, USA). Then, 1 μg of RNA was reverse transcribed into cDNA using Superscript III first-strand synthesis Supermix for qRT-PCR (Life Technologies, Carlsbad, CA, USA). Quantitative PCR was performed using a StepOnePlus™ real-time PCR system and a power SYBR® Green Master Mix (Life Technologies, Carlsbad, CA, USA) according to the manufacturer's instructions. The quantitative PCR reaction consisted of 10 μL of the master mix (Life Technologies, Carlsbad, CA, USA), 1 μL of primers (0.4 μM) and 1 μL of cDNA in a final volume of 20 μL. The specific primer pairs used for amplification of the *ZSD1*, *ZSS1* and *CYP71BA1* transcripts were 5′-GCAAGTGATGGTGGAGCAAAA-3′ (forward), 5′-CCGGCTACTTGTGTTGGACGT-3′ (reverse), 5′-GCAAGTGATGGTGGAGCAAAA-3′ (forward), 5′-CC GAGCTACTTGTGTTGGACGT-3′ (reverse), 5′-AGCGTGC ATAAGCAACAAGTAC-3′ (forward) and 5′-TGAGTT CGGGCGAGTTGGAG-3′ (reverse), respectively. Amplification of the endogenous reference gene (ubiquitin) was carried out using the following primers: 5′-AAGGA GTGCCCCAACGCCGAGTG-3′ and 5′-GCCTTCTGGT TGTAGACGTAGGTGAG-3′. Each sample was analyzed in triplicate, and the results represent the normalized mean values and SD.

Molecular modeling of *ZSD1*

The 3D structures of the protein complexed with the ligands were generated with Molecular Operating Environment (MOE), version 2009.10 (Chemical Computing Group, Montreal, Canada) using the crystal structure of *P. peltatum* (−)-secoisolariciresinol dehydrogenase [29] (Protein Data Bank code 2BGK) as a template. A ligand-free structure was generated by minimizing structural energy in the Amber99 force field with the default parameters. For the *in silico* docking simulation, the atomic coordinate of 8-HAH was prepared with the MOE by energy-minimizing the drawn structures under MMFF94x forcefield [33,34]. The simulation to dock 8-HAH to the ZSD1 model structure was performed with MOE-ASEDOCK 2005 [35]. The ZSD1-8HAH complex model obtained was superimposed

with the GatDH-erythritol co-crystal structure using the MOE superpose program. The figures for the protein structure were generated with program PYMOL (Schrödinger, New York, NY, USA).

Generation of ZSD1 mutants

The following primer pairs were used to introduce point mutations into the ZSD1 ORF: Y155A forward, 5′-GC TGGTCCACATGGAGCAACGGGGGC AAAACATG-3′, and Y155A reverse, 5′-CATGTTTTGCCCCCGTTGCTC CATGTGGACCAGC-3′; K159A forward, 5′-GATAC ACGGGGGCAGCACATGCTGTAGTAG-3′, and K159A reverse, 5′-CTACTACAGCATGTGCTGCCCCCGTGTAT C-3′; S142A forward, 5′-CTATAGTCTCCCTGGCCGCA GTATCTTCTGTGATTG-3′, and S142A reverse, 5′-CAAT CACAGAAGATACTGCGGCCAGGGAGACTATAG-3′; S144A forward, 5′-CCTGGCCAGTGTAGCTTCTGTGAT TGC-3′, and S144A reverse, 5′-GCAATCACAGAAGCTA CACTGGCCAGG-3′. These primers were used with the pET-ZSD1 plasmid and the proofreading *Pfu*-turbo DNA polymerase (Agilent Technologies, Santa Clara, CA, USA) for PCR (94 °C for 1 min, followed by 18 cycles of 94 °C for 30 s, 55 °C for 1 min, 68 °C for 5 min). Subsequently, the PCR products were digested with *Dpn*I (Toyobo, Osaka, Japan) for 1 h at 37 °C, and 5 μL was used to transform *E. coli* strain JM109. The plasmids obtained from the transformants were purified and sequenced.

Acknowledgements

We thank Mr T. Ishida, Ms R. Sawa and Mr H. Miyawaki for providing the ginger plants. We also thank Professor Kazutoshi Shindo and Professor Morio Asaoka for their helpful advice. This work was supported in part by the Research and Development Program for New Bio-industry Initiatives (2006–2010) from the Bio-oriented Technology Research Advancement Institution (BRAIN).

References

1 Lechat-Vahirua I, Francois P, Menut C, Lamaty G & Bessiere MJ (1993) Aromatic plants of French Polynesia. I. Constituents of the essential oils of rhizomes of three zingiberaceae. Zingiber zerumbet Smith, Hedychium coronarium Koenig and Etlingera cevuga Smith. *J Essent Oil Res* **5**, 55–59.

2 Dung NX, Chinh TD, Rang DD & Leclercq PA (1993) The constituents of the rhizome oil of *Zingiber zerumbet* (L.) Sm. from Vietnam. *J Essent Oil Res* **5**, 553–555.

3 Srivastava AK, Srivastava SK & Shah NC (2000) Essential oil composition of *Zingiber zerumbet* (L.) Sm. from India. *J Essent Oil Res* **12**, 595–597.

4 Chene-Ming J, Vera R & Chalchat JC (2003) Chemical composition of the essential oil from rhizomes, leaves and flowers of *Zingiber zerumbet* Smith from Reunion Island. *J Essent Oil Res* **15**, 202–205.

5 Bhuiyan MNI, Chowdhury JU & Begum J (2009) Chemical investigation of the leaf and rhizome essential oils of *Zingiber zerumbet* (L.) Smith from Bangladesh. *Bangl J Pharmacol* **4**, 9–12.

6 Ozaki Y, Kawahara N & Harada M (1991) Anti-inflammatory effect of *Zingiber cassumunar* Roxb. and its active principles. *Chem Pharm Bull (Tokyo)* **39**, 2353–2356.

7 Kirana C, McIntosh GH, Record IR & Jones GP (2003) Antitumor activity of extract of *Zingiber aromaticum* and its bioactive sesquiterpenoid zerumbone. *Nutr Cancer* **45**, 218–225.

8 Murakami A, Takahashi D, Kinoshita T, Koshimizu K, Kim HW, Yoshihiro A, Nakamura Y, Jiwajinda S, Terao J & Ohigashi H (2002) Zerumbone, a Southeast Asian ginger sesquiterpene, markedly suppresses free radical generation, proinflammatory protein production, and cancer cell proliferation accompanied by apoptosis: the alpha,beta-unsaturated carbonyl group is a prerequisite. *Carcinogenesis* **23**, 795–802.

9 Murakami A, Tanaka T, Lee JY, Surh YJ, Kim HW, Kawabata K, Nakamura Y, Jiwajinda S & Ohigashi H (2004) Zerumbone, a sesquiterpene in subtropical ginger, suppresses skin tumor initiation and promotion stages in ICR mice. *Int J Cancer* **110**, 481–490.

10 Sakinah SA, Handayani ST & Hawariah LP (2007) Zerumbone induced apoptosis in liver cancer cells via modulation of Bax/Bcl-2 ratio. *Cancer Cell Int* **7**, 4.

11 Xian M, Ito K, Nakazato T, Shimizu T, Chen CK, Yamato K, Murakami A, Ohigashi H, Ikeda Y & Kizaki M (2007) Zerumbone, a bioactive sesquiterpene, induces G2/M cell cycle arrest and apoptosis in leukemia cells via a Fas- and mitochondria-mediated pathway. *Cancer Sci* **98**, 118–126.

12 Croteau RB, Davis EM, Ringer KL & Wildung MR (2005) (-)-Menthol biosynthesis and molecular genetics. *Naturwissenschaften* **92**, 562–577.

13 Gershenzon J, Maffei M & Croteau R (1989) Biochemical and histochemical localization of monoterpene biosynthesis in the glandular trichomes of spearmint (*Mentha spicata*). *Plant Physiol* **89**, 1351–1357.

14 Yu F, Okamto S, Nakasone K, Adachi K, Matsuda S, Harada H, Misawa N & Utsumi R (2008) Molecular cloning and functional characterization of α-humulene synthase, a possible key enzyme of zerumbone biosynthesis in shampoo ginger (*Zingiber zerumbet* Smith). *Planta* **227**, 1291–1299.

15 Yu F, Okamoto S, Harada H, Yamasaki K, Misawa N & Utsumi R (2011) *Zingiber zerumbet* CYP71BA1 catalyzes the conversion of alpha-humulene to 8-hydroxy-

alpha-humulene in zerumbone biosynthesis. *Cell Mol Life Sci* **68**, 1033–1040.
16 Jornvall H, Persson B, Krook M, Atrian S, Gonzalez-Duarte R, Jeffery J & Ghosh D (1995) Short-chain dehydrogenases/reductases (SDR). *Biochemistry* **34**, 6003–6013.
17 Kallberg Y, Oppermann U, Jornvall H & Persson B (2002) Short-chain dehydrogenases/reductases (SDRs). *Eur J Biochem* **269**, 4409–4417.
18 de Kraker JW, Franssen MC, Dalm MC, de Groot A & Bouwmeester HJ (2001) Biosynthesis of germacrene A carboxylic acid in chicory roots. Demonstration of a cytochrome P450 (+)-germacrene a hydroxylase and NADP+-dependent sesquiterpenoid dehydrogenase(s) involved in sesquiterpene lactone biosynthesis. *Plant Physiol* **125**, 1930–1940.
19 Brosche M & Strid A (1999) Cloning, expression, and molecular characterization of a small pea gene family regulated by low levels of ultraviolet B radiation and other stresses. *Plant Physiol* **121**, 479–487.
20 Finsterbusch A, Lindemann P, Grimm R, Eckerskorn C & Luckner M (1999) Delta(5)-3beta-hydroxysteroid dehydrogenase from *Digitalis lanata* Ehrh. – a multifunctional enzyme in steroid metabolism? *Planta* **209**, 478–486.
21 Davis EM, Ringer KL, McConkey ME & Croteau R (2005) Monoterpene metabolism. cloning, expression, and characterization of menthone reductases from peppermint. *Plant Physiol* **137**, 873–881.
22 Ringer KL, Davis EM & Croteau R (2005) Monoterpene metabolism. Cloning, expression, and characterization of (–)-isopiperitenol/(–)-carveol dehydrogenase of peppermint and spearmint. *Plant Physiology* **137**, 863–872.
23 Polichuk DR, Zhang Y, Reed DW, Schmidt JF & Covello PS (2010) A glandular trichome-specific monoterpene alcohol dehydrogenase from *Artemisia annua*. *Phytochemistry* **71**, 1264–1269.
24 Ryden AM, Ruyter-Spira C, Litjens R, Takahashi S, Quax W, Osada H, Bouwmeester H & Kayser O (2010) Molecular cloning and characterization of a broad substrate terpenoid oxidoreductase from *Artemisia annua*. *Plant Cell Physiol* **51**, 1219–1228.
25 Cankar K, van Houwelingen A, Bosch D, Sonke T, Bouwmeester H & Beekwilder J (2011) A chicory cytochrome P450 mono-oxygenase CYP71AV8 for the oxidation of (+)-valencene. *FEBS Lett* **585**, 178–182.
26 Takahashi S, Yeo YS, Zhao Y, O'Maille PE, Greenhagen BT, Noel JP, Coates RM & Chappell J (2007) Functional characterization of premnaspirodiene oxygenase, a cytochrome P450 catalyzing regio- and stereo-specific hydroxylations of diverse sesquiterpene substrates. *J Biol Chem* **282**, 31744–31754.
27 Choi HW, Lee BG, Kim NH, Park Y, Lim CW, Song HK & Hwang BK (2008) A role for a menthone reductase in resistance against microbial pathogens in plants. *Plant Physiol* **148**, 383–401.
28 Mayoral JG, Nouzova M, Navare A & Noriega FG (2009) NADP+-dependent farnesol dehydrogenase, a corpora allata enzyme involved in juvenile hormone synthesis. *Proc Natl Acad Sci USA* **106**, 21091–21096.
29 Youn B, Moinuddin SG, Davin LB, Lewis NG & Kang C (2005) Crystal structures of apo-form and binary/ternary complexes of Podophyllum secoisolariciresinol dehydrogenase, an enzyme involved in formation of health-protecting and plant defense lignans. *J Biol Chem* **280**, 12917–12926.
30 Carius Y, Christian H, Faust A, Zander U, Klink BU, Kornberger P, Kohring GW, Giffhorn F & Scheidig AJ (2010) Structural insight into substrate differentiation of the sugar-metabolizing enzyme galactitol dehydrogenase from *Rhodobacter sphaeroides* D. *J Biol Chem* **285**, 20006–20014.
31 Oppermann UC, Filling C, Berndt KD, Persson B, Benach J, Ladenstein R & Jornvall H (1997) Active site directed mutagenesis of 3 beta/17 beta-hydroxysteroid dehydrogenase establishes differential effects on short-chain dehydrogenase/reductase reactions. *Biochemistry* **36**, 34–40.
32 Rosano C, Bisso A, Izzo G, Tonetti M, Sturla L, De Flora A & Bolognesi M (2000) Probing the catalytic mechanism of GDP-4-keto-6-deoxy-d-mannose epimerase/reductase by kinetic and crystallographic characterization of site-specific mutants. *J Mol Biol* **303**, 77–91.
33 Weiner SJ, Kollman PA, Case DA, Singh UC, Ghio C, Alagona G, Profeta S & Weiner P (1984) A new force field for molecular mechanical simulation of nucleic acids and proteins. *J Am Chem Soc* **106**, 765–784.
34 Halgren TA (1999) MMFF VII. Characterization of MMFF94, MMFF94s, and other widely available force fields for conformational energies and for intermolecular-interaction energies and geometries. *J Comput Chem* **20**, 730–748.
35 Goto J, Kataoka R, Muta H & Hirayama N (2008) ASEDock-docking based on alpha spheres and excluded volumes. *J Chem Inf Model* **48**, 583–590.

Supporting information

The following supplementary material is available:
Fig. S1. Comparison of deduced amino acid sequence of *ZSD1* with related functionally characterized SDRs.

This supplementary material can be found in the online version of this article.

Please note: As a service to our authors and readers, this journal provides supporting information supplied by the authors. Such materials are peer-reviewed and may be reorganized for online delivery, but are not copy-edited or typeset. Technical support issues arising from supporting information (other than missing files) should be addressed to the authors.